Experimental Characterization of Hohlraum Conditions by X-Ray Spectroscopy

C. A. Back *B. F. Lasinski* *L. J. Suter*

E. J. Hsieh *B. J. MacGowan* *G. F. Stone*

R. L. Kauffman *L. V. Powers* *R. E. Turner*

T. D. Shepard

Introduction

Spectroscopy is a powerful technique used to measure the plasma parameters relevant to Inertial Confinement Fusion (ICF) plasmas. For instance, the onset of spectral signals from multilayer targets have been used to determine ablation rate scalings.[1] Temperature and density measurements in coronal plasmas have enabled the study of laser coupling efficiency as a function of the laser wavelength.[2] More recently, dopants have been successfully used to determine capsule conditions of ICF targets.[3] However, few spectroscopic studies have been performed to diagnose plasma conditions of the hohlraum itself. Several laboratories have studied enclosed cavities,[4] previously concentrating on measurements of the radiative heat wave, the x-ray conversion efficiency, and temporal evolution of Au x rays. Measurements of electron temperature T_e and electron densities n_e are difficult because many physical processes occur and each diagnostic's line-of-sight is restricted by the hohlraum wall. However, they are worth pursuing because they can provide critical information on the target energetics and the evolution of plasma parameters important to achieving fusion.

In this article, we discuss spectroscopic tracers to diagnose plasma conditions in the hohlraum, using time- and space-resolved measurements. The tracers are typically mid-Z elements (Z = 13–24), which are placed on the hohlraum wall or suspended in the hohlraum volume. To demonstrate the breadth of measurements that can be performed, three types of experiments are presented. The first set tests ablation inside hohlraums by using tracers under the laser beam focal spot. The second set examines the heating of the wall by the tracers buried at different depths. The third set measures T_e by analysis of line intensity ratios. Spectroscopy has an advantage over imaging studies because it can provide nonperturbative measurements of local plasma parameters, i.e., T_e and n_e. Furthermore, not only can a spectra allow a measurement of plasma conditions, but its temporal behavior can reveal information about the hydrodynamics and heating of the hohlraum.

Experimental Approach

Microdots aid the spectroscopic analysis by limiting optical depth, localizing the tracer, and reducing edge effects of laser irradiation.[5] Target fabrication techniques successfully produce versatile hohlraums having tracer dopants deposited as high-precision microdots or strips. The tracers are deposited on a thin substrate such as an 800-Å CH foil or on a 25-µm-thick Au foil that mimics the hohlraum wall. The advantages of using tracers for probing the plasma include: (1) creating a localized plasma to track the dopant by emission or absorption, (2) controlling the thickness of the dopant, (3) systematically varying the depth of the tracer to probe different layers below the surface, and (4) defining the transverse plasma length probed to produce optically thin transitions. These advantages are important to successfully diagnose the complex hohlraum environment. LASNEX simulations of plasmas created from tracers indicate that the plasma can remain localized inside the hohlraum. For instance, different positions of the density gradient can be probed by suitably choosing the depth at which a tracer is buried.[6] Thus the experiments can be particularly effective in understanding ablation, plasma formation in nonplanar geometries, and overall energy balance.

UCRL-LR-105821-95-3

Since the plasmas may be >1 mm, the accuracy of spectroscopic measurements have benefited from the development of x-ray streak cameras and gated imagers. Streak cameras provide continuous temporal resolution of the spectral signal while gated imagers allow imaging of the spectra produced from a microdot or strip. Recently, we developed and fielded a spectrograph using a Bragg x-ray diffraction crystal coupled to a gated module,[7] which converts one dimension of the spatial resolution to spectral resolution. Its primary advantage over other diagnostics is that it *spectrally* images x-ray emission from laser-produced targets in 250 ps time frames. These technological developments have been essential to achieve sufficient spatial and spectral resolution of these targets.

Experimental Results

Figure 1 is a schematic of the target showing the placement of tracer foils. Tracers are placed on the wall for ablation and wall heating experiments, as indicated in the figure. Tracers are deposited on a free-standing foil that is suspended inside the hohlraum for recent experiments measuring the T_e of gas-filled targets, also shown in the figure. This section discusses three types of experiments that can be performed: ablation measurements, embedded microdot emission measurements, and T_e measurements.

Ablation Measurements

In ablation experiments, we compared a lined and unlined hohlraum by monitoring the emission of KCl that was deposited on a Au foil on the hohlraum's inside surface. The KCl was directly irradiated by a laser beam and observed with x-ray streak cameras. The dot provided spectral signals that served as a temporal marker of the laser incident on the hohlraum's inside surface.

The targets were scale-1 hohlraums that were either lined with 7500 Å of CH or unlined. At the position of beamline 6, a hole was drilled into the hohlraum and covered with a foil patch with the KCl facing the inside of the hohlraum. The patch consisted of a 25-μm Au foil overcoated with 3500 Å of KCl. Eight Nova beams at $3\omega_o$ irradiated the target in the standard pointing and focusing geometry to produce focal spots on the hohlraum wall ~550 μm × 900 μm diam. The total laser energy was 22.3 kJ with <5% variation. In a 1 ns square pulse, this produces an intensity of 6×10^{14} W/cm^2 in each focal spot.

Figure 2 shows an example of the data. Line intensity traces as a function of time were taken for the He-like α line (n = 2–1) of Cl, $1s^2$ ($^1S_0$) –1s2p ($^1P_1$). For comparison, the Au emission was taken as close as possible to the short wavelength side of the line to minimize differences in detector response and to avoid the Cl satellites.

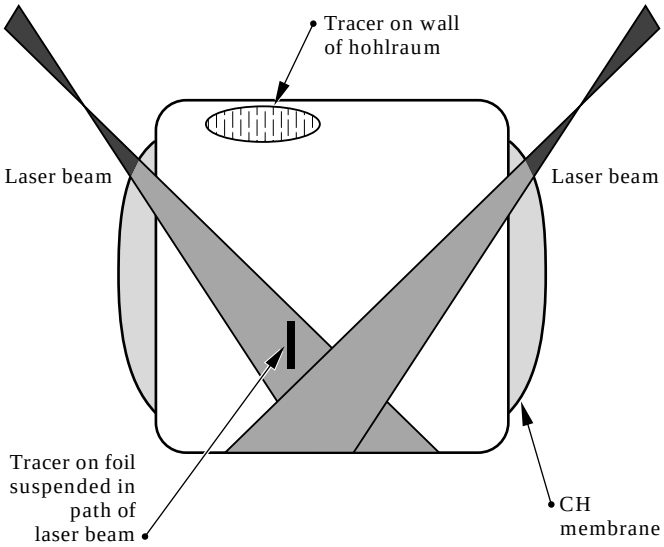

FIGURE 1. Schematic of a hohlraum target showing the position of patches and suspended foils. (08-20-0695-1660pb01)

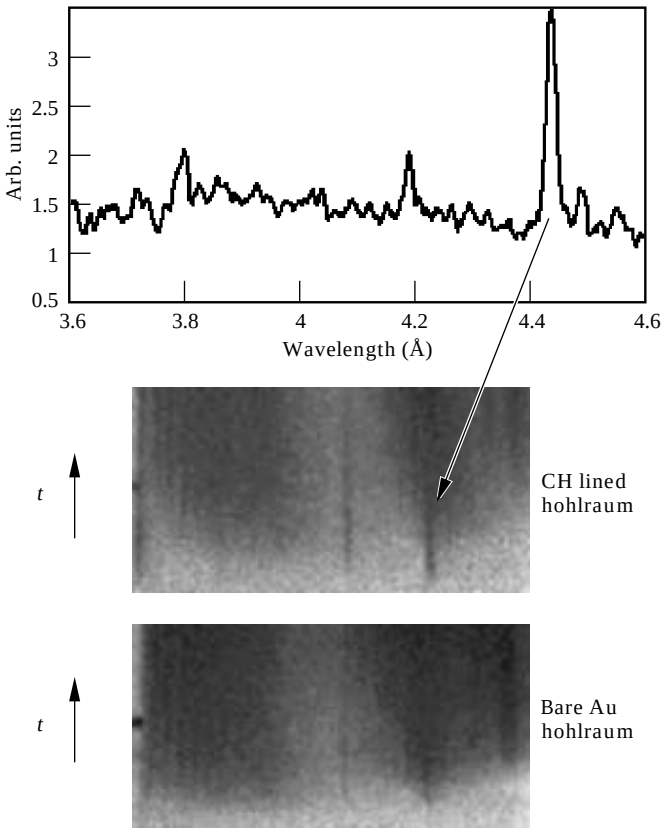

FIGURE 2. Example of data and a lineout from ablation experiments. (08-20-0695-1661pb01)

Figure 3 compares these four traces. There are two salient features of the temporal evolution. Early in time, the slope of the emission can be approximated by a straight line for all the lineouts. Later in time, the slope changes abruptly for all the cases except the Au emission from the lined hohlraum.

We define the burnthrough time as the temporal delay between the Cl emission from the tracer and Au emission from the lined or unlined hohlraum. In the unlined case, the KCl burns through and Au emission is detected 40 ps later when comparing the half maximum intensity. The lined case shows burnthrough to the Au 100 ps later. The onset of the signal taken is $t = 0$, where we assume that the delay in ionizing to He-like Cl is negligible. Here, the relative difference in the Au vs Cl emission is more important than the absolute value of the timing. The reference intensity for each case is the intensity when the KCl signal is no longer distinct from the Au signal. The difference reveals that there is a lag of 60 ps between the lined and unlined case.

A noticeable shoulder in the data exists where the slope of the intensity changes. Initially, the KCl in both the unlined and lined case follow the same curve, then their evolutions differ. If we consider the KCl as only a timing marker, the delay in burnthrough, as determined from the relative time lag of Au emission, is 80 ps. This delay has physical significance since the KCl foil was *not* overcoated with 7500 Å of CH and is therefore exactly the same in the two cases.

Because the intensity of the Cl emission is identical for the first 40 ps of emission, it is consistent to interpret the departure of the Cl slope as the inability of the laser to continue to heat the KCl in the CH lined hohlraum in the same way as the KCl in the unlined hohlraum. In addition, the intensity of the unlined and lined cases are different by a factor of two after 600 ps. Although the unlined and lined data are from two different experiments, the shots were performed on the same day, the target setup and spectrometer were identical, and differences due to film processing are minimal. Ablated CH inside of the hohlraum would produce a negligible attenuation of the signal. Therefore, the difference in intensity would indicate that less emission is detected in the lined hohlraum from both Au and Cl than from the unlined hohlraum.

Another measure of the target ablation is the time at which the KCl emission is no longer distinct from the Au emission. For the lined hohlraums, a detectable KCl signal persists for a longer period of time, 470 ps vs 280 ps. The duration of the KCl signal can be correlated with the amount of time that the KCl is localized enough to produce a signal above the Au background. When the KCl is no longer discernible from the Au, the total signal of the lined hohlraum is 70% of the unlined signal. When the KCl contribution is subtracted from the Au signal, the peak intensity of the lined hohlraum is 85% of the unlined signal. The result implies that the CH lined hohlraum has a slower ablation rate and does not cause Au emission of equal intensity within the first 600 ps of the laser pulse.

The measure of the burnthrough rate shows a measurable delay in time corresponding to ~80 ps. However, intensity of the Au emission is markedly different in both magnitude and evolution. Clearly at 600 ps, the Au has roughly half the integrated intensity, and the projection of the slope of the intensity vs time indicates that even after 1 ns, the Au emission of the lined hohlraum may not reach that of the unlined hohlraum.

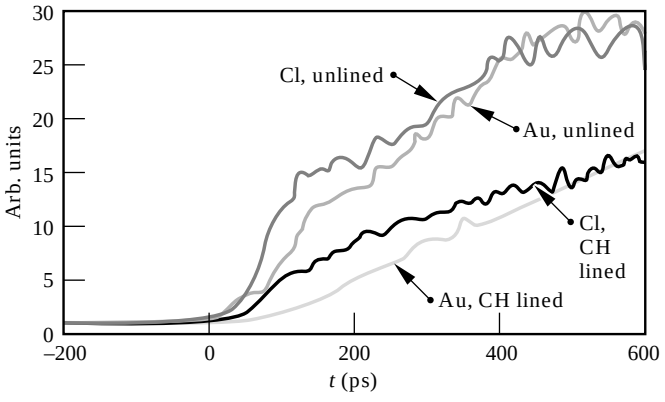

FIGURE 3. Comparison of the emission from Fig. 2.
(08-20-0695-1662pb01)

Embedded Microdot Hohlraum Experiments

Embedded microdot hohlraum experiments employed tracers buried under CH at a depth of 1 to 3 μm. The tracers were 250-μm-diam microdots of cosputtered Ti and Cr placed under a laser focal spot in a 3.2-mm-long hohlraum. Analysis of the spectra allowed us to examine heating of the inside hohlraum wall under a laser focal spot. Figure 4 shows an example of a TiCr K-shell spectrum where there is no appreciable H-like Cr. The top graph of Fig. 4 shows the laser pulse used to heat the hohlraum. The emission becomes detectable by a gated spectroscopic imager only ~2.2 ns after the beginning of the shaped pulse. Contrary to expectations, the tracer plasma does not become more ionized as the laser intensity increases to its peak. Calculations from foil burnthrough targets predict an T_e of ~2.5 keV. Due to the absence of H-like Cr in the experimental data, we conclude that the plasma remains less ionized than expected during the laser pulse. Based on the intensity of the He-like β resonance lines (n = 3–1) of Ti and Cr, the temperature derived from the isoelectronic sequence ratio is <2 keV. The spectra are 5% wider than the experimental width,

which indicates that line broadening or source motion may also be occurring. The late time spectrum shows the return of the Cr He-like β line, which probably indicates that recombination is occurring. Because the tracer plasma was cooler than expected and the TiCr spectral lines were weak, we can only infer an estimate of the T_e from the data. The most plausible explanation for the discrepancy between calculations and experiments is that the tracer dot remains well localized and moves out of the laser beam path, thereby sampling a cooler plasma.

T_e Measurements

We designed this set of experiments to measure the T_e of gas-filled hohlraum targets. The target was a 2.5-mm-diam and 2.5-mm-long Au hohlraum. To confine the gas, all openings were covered with thin polyimide windows (1 μm thick over the diagnostic holes, 6000 Å thick over the laser entrance holes). The hohlraum was filled with neopentane gas C_5H_{12} and

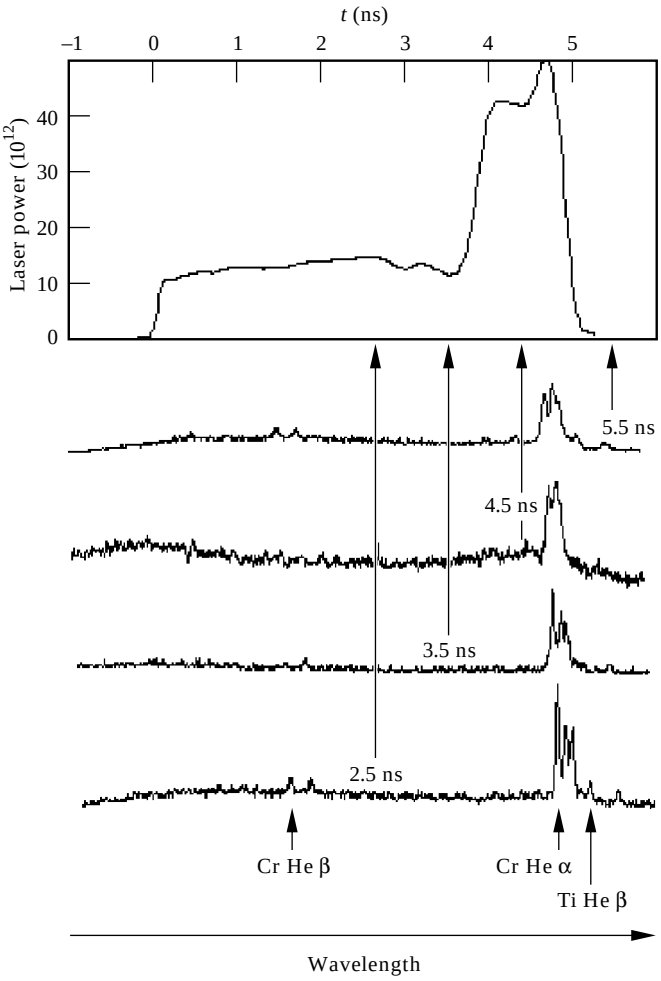

FIGURE 4. Data from a CH lined hohlraum showing a tracer embedded at 1 μm. (08-20-0695-1663pb01)

was designed to create a large millimeter-size plasma for stimulated Brillouin scattering and stimulated Raman scattering studies.[8]

These hohlraums are smaller than those used in the previous experiments and are expected to have a higher radiation temperature T_R. In the presence of an intense external photon flux, the ionic populations become more difficult to calculate because the introduction of the radiative transfer requires a solution of an integrodifferential equation which depends on the population and the field. Previous spectroscopic diagnostics cannot be extrapolated to these cases because they do not include the effects of an intense photon field. In the smaller hohlraums, the T_R can be high enough to actively perturb the level populations of the dopants and thereby will change the standard dependencies of these level populations on the T_e and n_e. This means that the ratios will now have an added dependence on the radiation field, which was previously assumed negligible. This radiation field will tend to deplete lower level populations by photoionization and photoexcitation and will cause mixing between excited levels, as they thermalize with the radiation field. Since these effects depend on the population and depopulation of energy levels, which are intricately coupled to the radiation field, and the plasma response to that photon field, the ratios will depend not only on the T_R, but on the *detailed spectral structure* of the radiation field.

To analyze the spectra from gas-filled hohlraums, the radiation field generated inside the 2.5-mm-diam hohlraums was measured by an x-ray diode diagnostic called Dante.[9] These experiments provided data that were used as input to the spectroscopic plasma models. Figure 5 shows the spectra of the radiation drive obtained at the peak of the pulse. Overall, the peak T_R was ~190 eV. In the experiments, the diagnostic observed

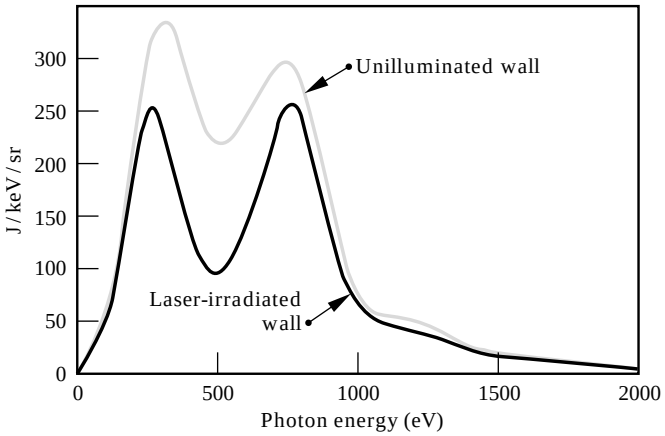

FIGURE 5. Dante spectra of the flux from a 2.5-mm-diam hohlraum at the peak intensities generated during the pulse. M bands are not shown. (08-20-0695-1665pb01)

either a beam focal spot or an area that was not irradiated by the beam. The measurements allow a comparison of the frequency dependence of the radiation field for these two cases. As shown in Fig. 5, both spectra are non-Planckian and there is a marked difference in the relative intensities of the O and N spectral bands. In general, measurements observing a laser focal spot on the wall have more pronounced N and M bands. For the T_R measured in these types of targets, the radiation effects on the spectra are not significant enough to affect the temperature measurements. This effect does become important in targets with higher T_R and research in this area continues.

FIGURE 6. Photograph of a foil suspended in a hohlraum target. (10-00-0394-0788Apb01)

To measure the T_e in these hohlraums, a tracer plasma was formed from a 2000 Å deposit of Ti and Cr cosputtered onto a 800 Å thick CH foil substrate. Figure 6 is a photograph of the target, which shows a vertical foil suspended in the hohlraum. The measurement is based on a technique which uses isoelectronic lines from ionized plasmas to diagnose T_e.[10] Briefly described, it is a line intensity ratio of emission from the same transition originating from two different ionic species having the same ionization stage. For instance, in this case we use the Cr He β resonance line, $1s^2\ (^1S_0) - 1s3p\ (^1P_1)$, and the Ti He β resonance line.

Because of the potential nonuniformity of the inside of the hohlraum, the tracer is deposited in a 100-μm-wide strip that is suspended in the hohlraum with the deposit facing the beam, as shown in Fig 1. Figure 7 shows an example of the spectra that have been corrected for the instrument response and gain. The experimental data, represented by circles in Fig. 8, show that $T_e \geq 3$ keV for 500 ps. The full results and other experimental details of the measurements will be reported elsewhere.[11]

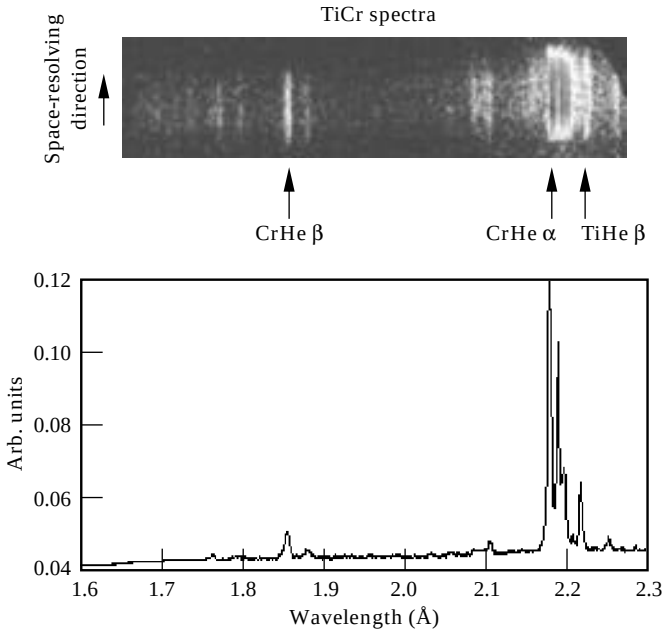

FIGURE 7. Data and lineout of the x-ray emission from a hohlraum target. (08-20-0695-1664pb01)

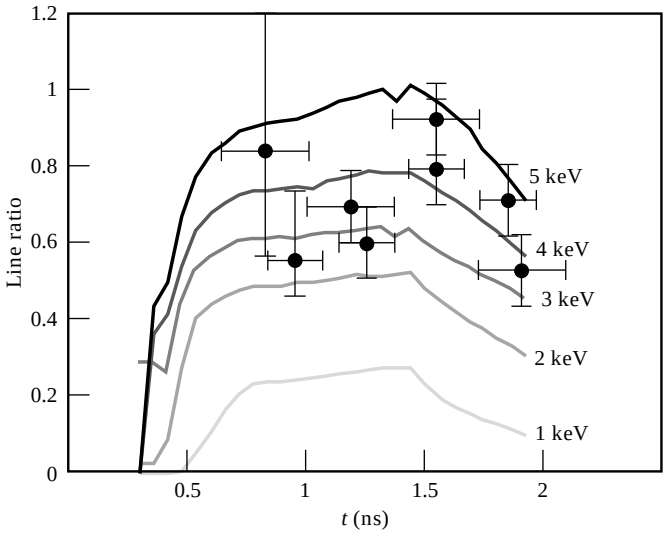

FIGURE 8. Example of data from a hohlraum target. (08-20-0895-1871pb01)

Summary

To achieve fusion by indirect drive, a confined cavity creates an x-ray source to provide proper symmetry for the implosion of a microballoon. The experiments described here are designed to diagnose the hohlraum plasma conditions by spectroscopy. The detailed behavior of hohlraums can be explored by these techniques because tracers can diagnose the *local* plasma conditions.

Experiments have demonstrated that line emission from microdot tracer plasmas can be observed above background emission. Emission from dopants on the hohlraum wall have revealed that spectra obtained from lined hohlraums have a temporal delay and are not as intense as those of unlined hohlraums. Recent results from lined and gas-filled hohlraums have shown that the T_e can be diagnosed by a line intensity ratio technique. Large lined hohlraums achieve temperatures of <2 keV while gas-filled 2.5-mm hohlraums reach T_e > 3 keV. Near-term experiments will develop the spectroscopic techniques to test the effect of high radiative fluxes on the plasma kinetics models and will explore the time-dependent effects.

Notes and References

1. W. C. Mead, et al., *Phys. Fluids* 26, 2316 (1993).
2. H. Pepin, R. Fabbro, B. Farai, F. Amiranoff, et al., *Phys. Fluids* 28, 3393 (1985); D. Phillion and C. J. Hailey, *Phys. Rev. A* 34, 4886 (1986).
3. C. L. S. Lewis and J. McGlinchey, *Opt. Commun.* 53, 179 (1985); A. Hauer, R. D. Cowan, B. Yaakobi, O. Barnouin, and R. Epstein, *Phys. Rev. A* 34, 411 (1986); B. A Hammel et al., *Phys. Rev. Lett.* 70, 1263 (1993).
4. B. Thomas, S. J. Davidson, C. C. Smith, and K. A. Warburton, ACO-UK-7839, 1985; R. Sigel, et al., *Phys. Rev. Lett.* 65, 587 (1990); R. Weber, P. F. Cunningham, and J. E., *Appl. Phys. Lett.* 53, 2596 (1988); R. L. Kauffman, et al., *Phys. Rev. Lett.* 73, 2320 (1994); H. Nishimura, H. Takabe, K. Kondo, T. Endo, et al., *Phys. Rev. A* 43, 3073 (1991).
5. P. G. Burkhalter, M. J. Herbst, D. Duston, J. Gardner, et al., *Phys. Fluids* 26, 3650 (1983); M. J. Herbst, P. G. Burkhalter, J. Grun, R. R. Whitlock, and M. Fink, *Rev. Sci Instrum.* 53, 1418 (1982); J. J. Herbst and J. Grun, *Phys. Fluids* 24, 1917 (1981).
6. T. Shepard, Lawrence Livermore National Laboratory, Livermore, CA, private communication (1994).
7. C. A. Back, R. L. Kauffman, P. M. Bell, J. D. Kilkenny, *Rev. Sci. Instrum.* 66, 764 (1995).
8. L. V. Powers, et al., *Phys. Rev. Lett.* 74, 2957 (1995).
9. H. N. Kornblum, R. L. Kauffman, and J. A. Smith, *Rev. Sci. Instrum.* 57, 2179 (1986).
10. T. D. Shepard, C. A. Back, B. H. Failor, W. W. Hsing, et al., *ICF Quarterly Report* 4(4), 137–144, Lawrence Livermore National Laboratory, Livermore, CA, UCRL-LR-105821-94-4 (1994).
11. C. A. Back, D. H. Kalantar, B. J. MacGowan, R. L. Kauffman, et al., "Measurements of Electron Temperature by Spectroscopy in Millimeter-Size Hohlraum Targets," Lawrence Livermore National Laboratory, Livermore, CA, UCRL-JC-122046 (in progress, 1995), in preparation for *Phys. Rev. Lett.*